Effect of chemical composition on hot cracking susceptibility (HCS) using various hot cracking criteria

Pujiyulianto, E.; Suyitno; Rajagukguk, K.; Arifvianto, B.; Katgerman, L.; Paundra, F.; Yudistira, H. T.; Nurullah, F. P.; Muhyi, A.; Arif, M. F.

DOI
10.1016/j.engfailanal.2023.107501

Publication date
2023

Document Version
Final published version

Published in
Engineering Failure Analysis

Citation (APA)
Pujiyulianto, E., Suyitno, Rajagukguk, K., Arifvianto, B., Katgerman, L., Paundra, F., Yudistira, H. T., Nurullah, F. P., Muhyi, A., & Arif, M. F. (2023). Effect of chemical composition on hot cracking susceptibility (HCS) using various hot cracking criteria. *Engineering Failure Analysis*, *152*, Article 107501. https://doi.org/10.1016/j.engfailanal.2023.107501

Engineering Failure Analysis 152 (2023) 107501

Contents lists available at ScienceDirect

Engineering Failure Analysis

journal homepage: www.elsevier.com/locate/engfailanal

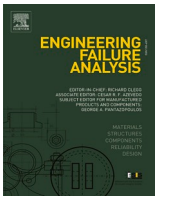

Effect of chemical composition on hot cracking susceptibility (HCS) using various hot cracking criteria

E. Pujiyulianto [a,d,*], Suyitno [b,d], K. Rajagukguk [a], B. Arifvianto [c,d], L. Katgerman [e,f], F. Paundra [a], H.T. Yudistira [a], F.P. Nurullah [a], A. Muhyi [a], M.F. Arif [g]

[a] Mechanical Engineering, Institut Teknologi Sumatera (ITERA), South Lampung, Lampung 35365, Indonesia
[b] Department of Mechanical Engineering, Faculty of Engineering, Universitas Tidar (UNTIDAR), North Magelang, Central Java 56116, Indonesia
[c] Department of Mechanical and Industrial Engineering Department, Engineering Faculty, Universitas Gadjah Mada (UGM), Yogyakarta 55281, Indonesia
[d] Center for Innovation of Medical Equipment and Devices (CIMEDs), Universitas Gadjah Mada (UGM), Yogyakarta 55281, Indonesia
[e] Department of Materials Science and Engineering, Delft University of Technology, Mekelweg 2, 2628CD Delft, the Netherlands
[f] Katgerman Aluminium Technology, van Beuningenlaan 10, 2334CC Leiden, the Netherlands
[g] Material Engineering, Institut Teknologi Sumatera (ITERA), South Lampung, Lampung 35365, Indonesia

ARTICLE INFO

Keywords:
Chemical composition
Hot cracking
Aluminum alloys
Critical temperature

ABSTRACT

The paper aims to evaluate the effect of chemical composition on the Hot Cracking Susceptibility (HCS) using mechanical and non-mechanical hot cracking criteria during solidification. The criteria were SKK as a mechanical criterion. Feurer, Clyne Davis, and Katgerman as non-mechanical criteria. The criteria were implemented at various parameters to evaluate their abilities in the hot cracking susceptibility (HCS) prediction at varied chemical composition. In this study, The Mg content was varied in Al9Zn (1, 1.5, 2, 2.5 %wt.) Mg2Cu alloys and Cu content in Al9Zn2Mg (1, 1.5, 2, 2.5 %wt.) Cu alloys. The validation of the result is also conducted by comparing with the experimental data. Based on Feurer criterion, The hot cracking initiates at lower temperature and at higher critical rate of feeding and shrinkage with Cu content, and the hot cracking initiates at higher temperature with Mg content, and it initiates at higher critical rate of feeding and shrinkage from 1 up to 1.5 of Mg, and the critical rate of feeding and shrinkage remains constant from 1.5 up to 2.5 of Mg. Based on Clyne & Davies, the HCS decreases with Cu content from 1 up to 2 of Cu, and it increases from 2 up to 2.5 of Cu. The HCS decreases with Mg content from 1 up to 2 of Mg, and it remains constant from 2 up to 2.5 of Mg. Based on Katgerman criterion, the HCS decreases with Cu content from 1 up to 1.5 of Cu, it increases from 1.5 up to 2 of Cu, and it decreases from 2 up to 2.5 of Cu. The HCS decreases sequentially with Mg content. Based on SKK criterion, the HCS curves shift to the right with Cu content which means that the hot cracking initiates at lower temperature, and the HCS curves shift to the left with Mg content which means that the hot cracking initiates at higher temperature with Mg content. The Feurer, Clyne & Davies, and some specific range for SKK criteria are in agreement for the effect of Cu content on HCS of alloys, and Katgerman and some specific range for Clyne&Davies criteria are in agreement for the effect of Mg content on HCS of alloys.

* Corresponding author.
E-mail address: eko.pujiyulianto@ms.itera.ac.id (E. Pujiyulianto).

https://doi.org/10.1016/j.engfailanal.2023.107501
Received 24 May 2023; Received in revised form 20 July 2023; Accepted 21 July 2023
Available online 23 July 2023

1. Introduction

Hot cracking, also known as hot tearing, hot brittleness, or solidification cracking [1–2], has been considered to be a severe trouble that often initiated during the solidification of metal such as in casting [1–4], and in welding [5–9]. It is a type of fracture that is initiated by the contraction of the molten metal when it solidifies, and it generates the high-tension stresses that exceed the strength of solidified metal, thus the crack will form. It might occur in the center, beneath of the surface, or in the surface of the metal [2]. Commonly, the hot cracking starts to initiate at the interdendritic separation stage during solidification where the liquid feeding occurs [1]. Nowadays, there are a lot of theories or criteria of the hot cracking that explain the hot cracking prediction as well as the initiation and the propagation during the solidification [10]. Currently, the hot cracking criteria are classified into mechanical, non-mechanical, and combined both mechanical and non-mechanical criteria. The mechanical criteria are based on the stress generated during solidification e.g., Novikov Criterion, Dickhaus Criterion, Lahaie & Bounchard Criterion, Langlais & Gruzleski Criterion, and William & Singer Criterion [11–15], based on strain e.g., Novikov Criterion, Magnin Criterion [11,15,16–18], and based on strain rate e.g., Prokhorov Criterion, RDG Criterion, Braccini Criterion, Stangeland Criterion, and Hamdi Criterion, [19–24]. The non-mechanicals are Feurer criterion, Clyne & Davies criterion, Modified Clyne & Davies Criterion, and Katgerman Criterion [2,25–26]. The combined mechanical and non-mechanical are SKK (Suyitno Kool Katgerman) and modified SKK criterion [27–28]. The criteria that well widely recognized due to their fitness and accuracy to some experimental parameters are Feurer, Clyne Davies, Katgerman [25–26], and SKK criterion [27–28]. Currently, the evaluations to get the proper model that can predict the initiation and the propagation of hot cracking during the solidification alloys, and the model that can fit to the experimental data at varied casting parameter e.g., chemical composition, strain rate, casting speed, pouring temperature, melting temperature, etc. are still counseled.

One of the crucial parameters that affect the hot cracking of metal alloys is the chemical composition. Several experimental studies have been conducted on evaluating of chemical composition on the Hot Cracking Susceptibility (HCS), whether for binary alloys [3,16], ternary alloys [29], and quaternary alloys [30]. The well-known result from experimental of hot cracking evaluation is the lambda curve. It is the satisfactory tool for evaluating and predicting the effect of chemical composition on the HCS based on the experimental studies. In contrast, theoretically, based on the hot cracking criteria, the research has not been conducted to evaluate the chemical composition effect on HCS using well-recognized hot cracking criteria. It is important to benchmarking the existing of hot cracking criteria to evaluate various hot cracking of alloys at varied composition. It would be useful for further research in the development of the hot cracking criteria as a function of chemical composition. For an industrial prospective, it would be applicable to know which of the criteria is close to the experimental data. It can be used for evaluating the susceptibility of alloys to hot cracking as a function of chemical composition, thus the failure of products can be avoided.

Based on the descriptions, this study aims to compare and to evaluate the chemical composition effect on Hot Cracking Susceptibility (HCS) of Al9Zn(1, 1.5, 2, 2.5)Mg2Cu alloys (wt%.) and Al9Zn2Mg(1, 1.5, 2, 2.5)Cu alloys (wt%.) using Feurer, Clyne & Davies, Katgerman, and SKK criteria. The validation of the data is conducted by comparing it to the experimental data. Some of the parameters that have been evaluated other than chemical composition by Clyne & Davies and Feurer are casting speed, by Katgerman are ingot diameter and casting speed, by SKK are casting speed, strain rate, cooling rate, packing parameter, grain diameter, and ramping procedure.

2. Mathematical model

2.1. Feurer criterion

Feurer criterion considers the feeding and shrinkage during solidification of metal alloys. The hot cracking is assumed due to the lack of feeding during solidification. It correlates to the difficulties of molten flow through the mush as a permeable medium in competition with the solidification shrinkage. Feurer considers *SPV* and SRG where the SPV is the maximum volumetric flow rate (feeding term) through a dendritic network as explained in Eqs. 1–3, and *SRG* is the volumetric solidification shrinkage as explained in Eqs. 4–5. As per Feurer's criterion, the hot cracking forms if $SPV < SRG$.

$$SPV = \frac{f_l^2 \lambda_2^2 P_s}{24\pi c^3 \eta L^2} \tag{1}$$

$$P_S = P_O + P_M - P_C \tag{2}$$

$$P_C = \frac{4\gamma_{SL}}{\lambda_2} \tag{3}$$

The f_l is volume fraction liquid, λ_2 is secondary dendrite arm spacing, P_s is effective feeding pressure, L is length of porous network, c is tortuosity constant of the dendritic network, η is viscosity of the liquid phase, γ_{SL} is solid liquid interfacial energy and P_O, P_M and P_C are atmospheric, metallostatic, and capillary pressure respectively.

$$SRG = \left(\frac{\partial \ln V}{\partial t}\right) = -\frac{1}{\overline{\rho}} \frac{\partial \overline{\rho}}{\partial t} \tag{4}$$

$$\overline{\rho} = \rho_l f_l + \rho_s f_s \tag{5}$$

The V is a volume element of the solidifying mush with constant mass, t is time,$\bar{\rho}$ is average density of the mush, ρ_l and ρ_s are densities of liquid and solid, respectively, and f_l and f_s are volume fractions liquid and solid in the dendritic network, respectively. Fig. 1 shows the critical point taken from the intersection curve between *SPV* and *SRG* during solidification. It indicates the boundary of sufficient and insufficient feeding conditions.

The critical temperature based on Feurer's criterion is expressed in terms of liquid fraction f_L where the *SPV* is equal to *SRG (SPV = SRG)*. It means that the insufficient feeding process during solidification is developed. When the solidification passes the critical temperature, the hot cracking initiates *(SPV < SRG)*.

2.2. Clyne & Davies criterion

Clyne & Davies state that the HCS is the ratio of vulnerable time (t_v) and the time where the mass feeding and the liquid feeding occur (t_R). The t_v is the subtraction of the time when the fraction of solid is 0.99 ($t_{0.99}$) with the time when the fraction of solid is 0.9 ($t_{0.9}$), and the t_R is the subtraction of the time when the fraction of solid is 0.9 ($t_{0.9}$) with the time when the fraction of solid is 0.4 ($t_{0.4}$).. The HCS as per Clyne & Davies criterion is explained by Eq.6 [25].

$$HCS = \frac{t_v}{t_R} = \frac{t_{0.99} - t_{0.9}}{t_{0.9} - t_{0.4}} \tag{6}$$

2.3. Katgerman criterion

The Katgerman criterion considers the time when the feeding process is inadequate (t_{cr}) and the time when the coherency points during the solidification (t_{coh}). The t_{cr} is determined from the intersection point of the curve between volumetric flow rate per unit volume *(SPV)* and shrinkage rate *(SRG)* as shown in Fig. 1. The value of t_{cr} is determined using Feurer's criterion, and is the time for which $SPV = SRG$, thus the *SPV* and *SRG* indicated by the intersection point as in Fig. 1. The HCS as per Katgemen criterion mathematically is stated in Eq.7 [26].

$$HCS = \frac{t_{0.99} - t_{cr}}{t_{cr} - t_{coh}} \tag{7}$$

2.4. SKK criterion

The SKK consists of three aspects namely the formation of cavities, the formation of thermal stresses in the mushy zone, and the hot cracking initiation and propagation. Those main parameters are explained below.

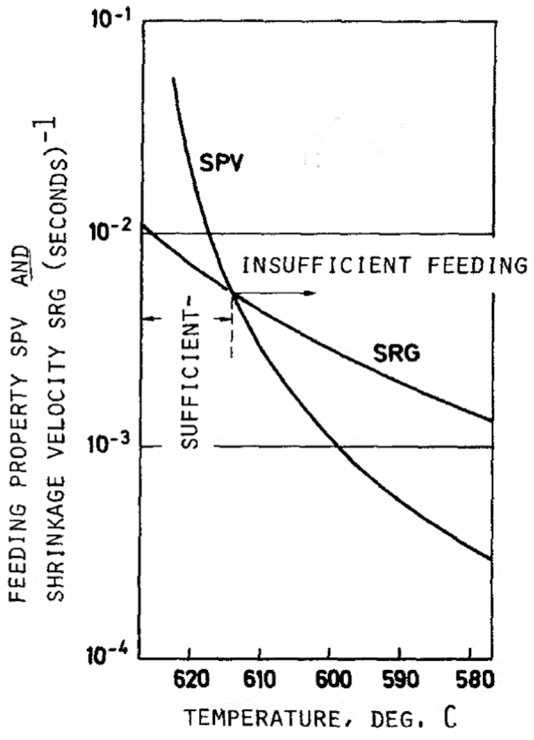

Fig. 1. Comparison of maximum volumetric flow rate (SPV) through the dendritic network and rate of solidification shrinkage (SRG) [33].

a. Solidification Model

The liquid fraction as a function of temperature is expressed in Eq. (8).

$$f_l = \frac{1}{1-2\alpha_s^* k}\left[\left(\frac{T_m - T}{T_m - T_l}\right)^{\frac{1-2\alpha_s^* k}{k-1}}\right] \text{and} \alpha_s^* = \alpha_s\left[1-\exp\left(-\frac{1}{\alpha_s}\right)\right] - \frac{1}{2}\exp\left(-\frac{1}{2\alpha_s}\right) \tag{8}$$

where T_m is the melting temperature of pure metal, T_l is the liquidus temperature, T is the temperature, k is the partition coefficient, α_s is the back-diffusion coefficient, and α_s^* is the modified dimensionless solid-state back diffusion parameter.

b. Evolution of cavity.

Mathematical equations to model the cavity formation based on the SKK criterion are expressed in Eqs. 9–10.

$$d = \left(\frac{3}{2\pi} f_v V_{char}\right)^{1/3} \tag{9}$$

$$V_{char} = c d_g^3 \tag{10}$$

where d is the cavity size, V_{char} is the characteristic volume of the local geometry (cavity and grains), and d_g is the diameter of the grain. c is a packing parameter of the grains, and it is equal to $2\sqrt{2}$ for *FCC*-like and $\frac{8}{3\sqrt{3}}$ for *BCC*-like, and f_v is the cavity volumetric fraction. The f_v in Eq. (8) is obtained using Eq. (11).

$$f_v = \int_{T_{crit}}^{T} \frac{\partial f_v}{\partial T} dT \tag{11}$$

c. Thermal stress in the mushy zone

The stress developed in the mush based on the SKK criterion is calculated using a constitutive model as expressed in Eq. (12).

$$\sigma = \sigma_o \exp(\beta f_s) \exp\left(\frac{mQ}{RT}\right) (\dot{\varepsilon})^m \tag{12}$$

where Q is the activation energy, m is the strain rate sensitivity coefficient, R is the gas constant, σ_o and β are material constants, and $\dot{\varepsilon}$ is the strain rate.

d. Hot cracking evaluation

SKK criterion used a Griffith's approach [31–32] to correlate the critical cavity length (a_{crit}) and the stress in the mush. The cavity propagates as a crack, and it is expressed in Eq. (13).

$$a_{crit} = 4\gamma_s \frac{E}{\pi\sigma^2} \tag{13}$$

where γ_s is the surface tension of the liquid metal, E is the young's modulus of the mush, and σ is the stress of the mush. Due to the irregularity of cavity shape, it needs to be considered its irregularity using Eq. (14) where the C_1 is the constant as shown in Table. 1.

$$a = C_1 d \tag{14}$$

Table 1
Parameter used in the calculations.

Parameter	Value	Unit	Ref.
A_s	0.01		[21]
k	0.14		[36]
T_m	933	K	[37]
σ_o	4.5	Pa	[22]
m	0.26		[22]
A	10.2		[22]
Q	160	kJ/mol	[22]
E	40	GPa	[27]
γ_{sl}	0.84	J/m^2	[38]
ρ_S	2790	kg/m^3	[38]
ρ_l	2480	kg/m^3	[38]
λ	8.10^{-5}	m	[27]
η	0.0013	Pa s	[38]
d_g	5.10^{-4}	m	[27]
C_1	1		[27]
C_2	$2\sqrt{2}$		[27]
$\dot{T}$	5	K/s	[38]
$\dot{\varepsilon}$	0.001		[38]

From Eqs. (13)–(14), both a_{crit} and a are compared. If $a \geq a_{crit}$, a crack will develop. The hot cracking susceptibility (HCS) as per SKK criterion is defined by Eq. (8).

$$HCS = \frac{a}{a_{crit}} \tag{15}$$

Qualitatively, the HCS will increase by increasing its value, and quantitatively, the hot cracking develops if the HCS is higher than 1.

2.5. Method of model implementation

The implementation of Feurer, Clyne & Davies, Katgerman, and SKK criteria were carried out by applying those criteria on the similar parameter process as shown in Table 1, and on some varied parameter such as the Cu composition on Al9Zn2Mg(1, 1.5, 2, 2.5% wt.)Cu alloys, and the Mg composition on Al9Zn(1, 1.5, 1, 2.5%wt.)Mg2Cu alloys.

The HCS values based on the Feurer, Clyne & Davies, Katgerman, and SKK criteria are compared and evaluated by normalized the HCS value. The normalized HCS values are classed to be extreme, high, moderate, and low HCS, and each class equal to 4, 3, 2, and 1, respectively. Finally, the results of the model implementation are validated by comparing to the experiment data as explained in Ref. [19,34–35].

3. Results and discussions

Fig. 2a-b show the cooling curve of alloys from 0.8 up to 1 of solid fraction. Fig. 2a for Al9Zn2Mg(1, 1.5, 2, 2.5%wt.)Cu alloys, and Fig. 2b for Al9Zn(1, 1.5, 2, 2.5%wt.)Mg2Cu. In Fig. 2a, it shows that the transformation point of 1, 1.5, 2, and 2.5 of Cu (%wt.) in Al9Zn2Mg(x)Cu occurs at $f_s = 0.89$, $T = 460.43$ °C, at $f_s = 0.87$, $T = 455.85$ °C, at $f_s = 0.85$, $T = 451.24$ °C, and at $f_s = 0.83$, $T = 445.76$ °C, respectively. It can be observed that the f_s and T at transformation point decreases with Cu content, and it states that the cooling curve and the transformation point shift to left and drop down a bit regularly with Cu content. In contrast as in Fig. 2b, it shows that the transformation point of 1, 1.5, 2, and 2.5 of Mg (%wt.) in Al9Zn(x)Mg2Cu occurs at $f_s = 0.89$, $T = 447$ °C, at $f_s = 0.87$, $T =$

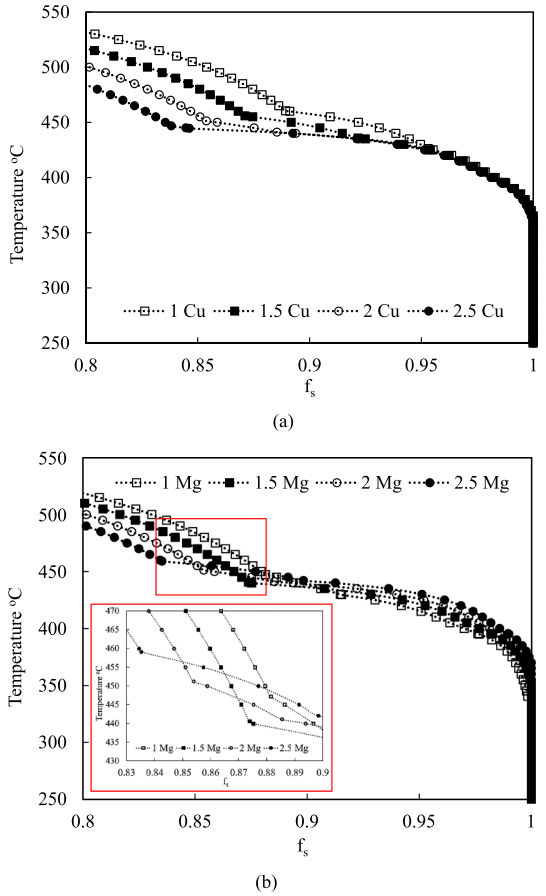

Fig. 2. Cooling curve of (a) Al9Zn2Mg(1, 1.5, 2, 2.5)Cu, and (b) Al9Zn(1, 1.5, 2, 2.5)Mg2Cu.

440 °C, at $f_s = 0.85$, $T = 450$ °C, and at $f_s = 0.83$, $T = 460$ °C, respectively. It can be observed that the f_s at transformation point decreases regularly with Mg content, and the T at transformation point decreases from 1 up to 1.5 of Mg (%wt.), and it increases from 1.5 up to 2.5 of Mg (%wt.). The cooling curve and the transformation point relate to the nucleation and phase growth during the solidification process.

Fig. 3a-b show the *SPV* and *SRG* curve. *SPV* is the volumetric flow rate per unit volume, and *SRG* is the shrinkage rate. In other terms, the *SPV* is the feeding process, and the *SRG* is the deformation process.

Fig. 3a-b show the intersection point of *SPV* and *SRG*. Fig. 3a for Al9Zn2Mg(1, 1.5, 2, 2.5%wt.)Cu alloys, and Fig. 3b for Al9Zn(1, 1.5, 2, 2.5%wt.)Mg2Cu alloys. The intersection points between *SPV* and *SRG* curve as shown in Fig. 3a-b indicate the critical temperature and the critical rate of feeding and shrinkage of each alloy during solidification. It occurs when the *SPV* is equal to *SRG (SPV = SRG)*. It means that the insufficient feeding process during solidification is developed. According to the Feurer criterion, the hot cracking occurs when the *SPV* < *SRG*. Fig. 3a shows that the intersection points between *SPV* and *SRG* curve shift to the right and go up a bit with Cu content, thus it states that the Cu content causes the hot cracking initiates at lower temperature and at higher critical rate of feeding and shrinkage. In Fig. 3b, the intersection points between *SPV* and *SRG* curve shift to the left with Mg content. The critical rate of feeding and shrinkage increases with Mg content in Al9ZnxMg2Cu from 1 up to 1.5 of Mg (%wt.), and the critical rate of feeding and shrinkage remains constant from 1.5 up to 2.5 of Mg (%wt.). It is concluded that the hot cracking initiate at higher temperature with Mg content, and the hot cracking initiates at higher critical rate of feeding and shrinkage from 1 up to 1.5 of Mg (%wt.), and the critical rate of feeding and shrinkage remains constant from 1.5 up to 2.5 of Mg (%wt.).

Fig. 3 shows an instability curve when experiencing the intersection point between the *SPV* and *SRG*, specifically near the critical temperature, or also known as rigidity temperature range [39]. Based on Ref. [39], it can be explained based on microscopic and mesomicroscopics phenomenon. Microscopically, it occurs due to the coherency phenomenon, and mesomicroscopically, it might happen due to lack of feeding, or stress, strain, or strain rate imposed on the structure [39]. During the rigidity temperature range, the permeability of the mush decreases jointly with shrinkage phenomenon, then the inadequate feeding be present that will cause the generation of nonuniform thermal stress which could be or could not be supported by the solid bridges. The limited access of the liquid

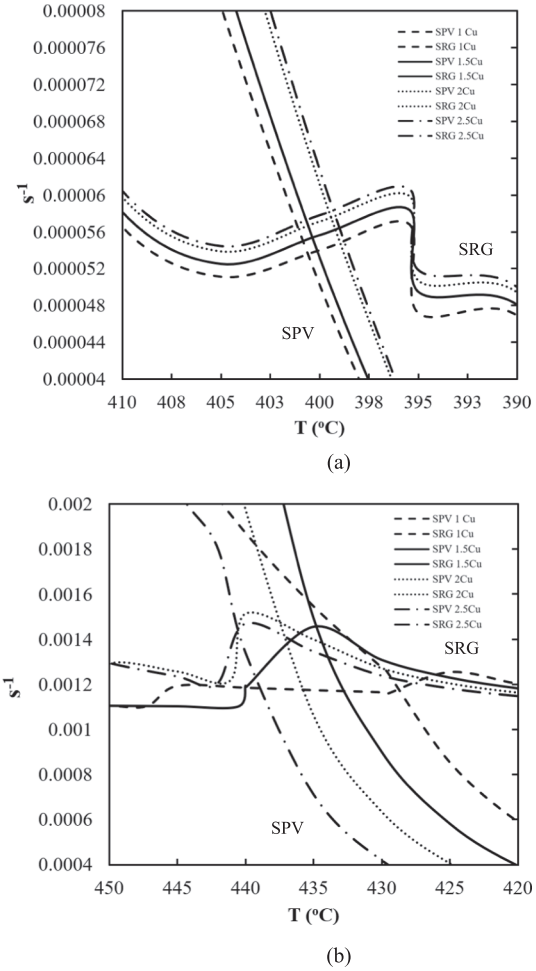

Fig. 3. Intersection point of *SPV* and *SRG* curve of (a) Al9Zn2Mg(1, 1.5, 2, 2.5%wt.)Cu, and (b) Al9Zn(1, 1.5, 2, 2.5%wt.)Mg2Cu.

to the solid bridge causes the brittle fracture. The mechanism is known as liquid–metal embrittlement [39]. Additionally, some Ref. [26] states that the stress resulting from inadequate feeding might be considered as the causes of hot tearing. In the other point of view, based on Ref. [40], the curve instability might be caused by the rate of dendrite growth to any direction before dendrite coherency point [40–42]. The multi direction of dendrite growth causes of solid fraction to increase at the dendrite coherency point range, so the interdendritic feeding would be intermitted [43].

Based on Feurer criterion, the critical temperature during solidification is when the $SPV = SRG$. Fig. 3 shows that the range of critical temperatures or rigidity temperatures for Al9Zn2Mg(1, 1.5, 2, 2.5%wt.)Cu are 399–402 °C (Fig. 3a), and for Al9Zn(1, 1.5, 2, 2.5%wt.)Mg2Cu are 427–443 °C (Fig. 3b). From Fig. 3, the critical or rigidity temperature can be plotted to get the value of f_s. It shows that the critical temperature for Al9Zn2Mg(1, 1.5, 2, 2.5%wt.)Cu occurs at f_s 0.96–0.98, and for Al9Zn(1, 1.5, 2, 2.5%wt.)Mg2Cu occurs at f_s 0.90–0.93. Based on Ref. [39], The temperature range or the solid fraction that the hot cracking might be initiated and propagated are classified into three assumptions [39]. Firstly, It is between coherency and rigidity temperature (50 up to 80 of solid fraction), or it is below the rigidity temperature (80 up to 99 of solid fraction), or it might be closed to the solidus (98 up to 100 of solid fraction). Based on the assumption above, the hot cracking based on the Feurer criterion correlates to the second statement that the hot cracking formed below the rigidity temperature (80 up to 99 of solid fraction).

Fig. 4a-b show the HCS curve based on Clyne & Davies criterion. Fig. 4a for Al9Zn2Mg(1, 1.5, 2, 2.5%wt.)Cu alloys, and Fig. 4b for Al9Zn(1, 1.5, 2, 2.5 %wt.)Mg2Cu alloys. Based on Fig. 4a, the HCS decreases with Cu content from 1 up to 2 of Cu (%wt.), and it increases from 2 up to 2.5 of Cu (%wt.). The results are in accordance with the experimental data as in Ref. [35] where the HCS decreases from 0 up to 2 of Cu (%wt.), and it increases from 2 up to 3 of Cu (%wt.) [35]. Based on Ref [35], the increase of Cu (%wt.) in Al-Zn-Mg-Cu alloys decreases the grain size, and it increases the eutectic phase in the boundary. When the grain size is smaller, the stress generated during solidification shrinkage at the dendrite skeleton becomes more dispersed, thus the tendency of grain boundary cracking or the HCS is also lower [35,4]. Nonetheless, the HCS increases with Cu content from 2 of Cu (%wt.). It occurs due to the divorced eutectic structure on the grain boundary [35]. Fig. 4b shows the effect of Mg content on HCS based on Clyne & Davies criterion. It states that the HCS decreases with Mg content from 1 up to 2 of Mg (%wt.), and it remains constant from 2 up to 2.5 of Mg (%wt.).

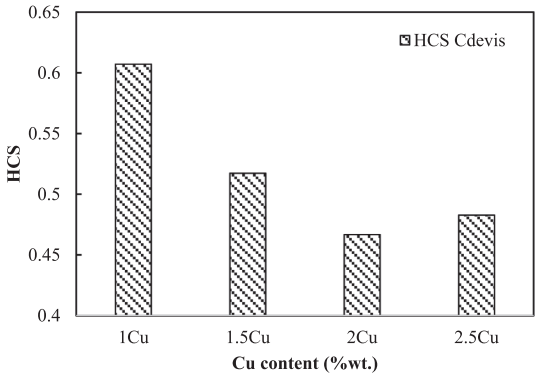

a)

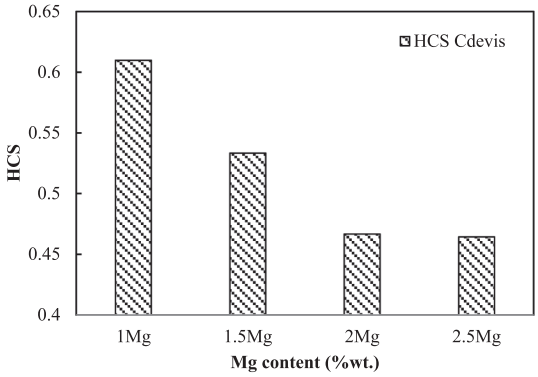

b)

Fig. 4. The HCS curve based on Clyne & Davies criterion, (a) Al9Zn2Mg(1, 1.5, 2, 2.5 %wt.)Cu, and (b) Al9Zn(1, 1.5, 2, 2.5 %wt.)Mg2Cu.

Fig. 5a-b show the HCS curve based on the Katgerman criterion. Fig. 5a for Al9Zn2Mg(1, 1.5, 2, 2.5 %wt.)Cu alloys, and Fig. 5b for Al9Zn(1, 1.5, 2, 2.5 %wt.)Mg2Cu alloys. Based on the Katgerman criterion, as shown in Fig. 4a, the HCS decreases with Cu content from 1 up to 1.5 of Cu (%wt.), it increases from 1.5 up to 2 of Cu (%wt.), and it decreases from 2 up to 2.5 of Cu (%wt.). Based on Katgerman criterion, the effect of Cu is fluctuated. It is not in agreement with experimental data as in ref. [35]. Fig. 4b shows that the HCS decreases sequentially with Mg content. Based on Ref. [41], the time range of Clyne & Davies criterion is correspondingly with HCS zone where the solid fraction interval varied between 0.90 and 0.99. At the same time, the Katgerman criterion uses the T_{cr} as the main parameter which is affected by the eutectic distribution, dendrite coherency, and solid fraction of pre-eutectic and near-eutectic compounds [41].

Fig. 6a-b show the HCS curve based on the SKK criterion. Fig. 6a for Al9Zn2Mg(1, 1.5, 2, 2.5%wt.)Cu alloys, and Fig. 6b for Al9Zn (1, 1.5, 2, 2.5%wt.)Mg2Cu alloys. Based on SKK criterion, the hot cracking initiates when the HCS is higher than 1 (HCS $>$ 1). Generally, Fig. 6a shows that the HCS curves shift to the right with Cu content which means that the hot cracking initiates at lower temperature. However, for 2 and 2.5 of Cu (%wt.), the curve is almost coincided. The results are in agreement with the experimental data as explained in Ref. [35] where the temperature of hot cracking initiation decreases from 0 up to 2 of Cu (%wt.), and it is almost constant from 2 up to 2.5 of Cu (%wt.). Fig. 6b shows that the HCS curve shifts to the left with Mg content which means that the hot cracking initiates at higher temperature with Mg content. Based on SKK, the effect of Cu and Mg content on Al-Zn-Mg-Cu has a contradiction effect.

Based on the discussion above, to ease for comparing and evaluating the HCS for each criteria as a function of chemical composition, The normalized of HCS values are implemented. It is shown in Fig. 7a-b.

Fig. 7a-b show the normalized of HCS value based on Feurer, Clyne and Davies, Katgerman, and SKK criteria. Fig. 7a for Al9Zn2Mg (1, 1.5, 2, 2.5%wt.)Cu alloys, and Fig. 7b for Al9Zn(1, 1.5, 2, 2.5%wt.)Mg2Cu alloys. In Fig. 7a, based on Feurer and SKK criteria, it shows that the normalized HCS value decreases with Cu content (%wt.), based on Clyne & Davies criterion, the normalized HCS value decreases from 1 up to 2 of Cu (%wt.), and it increases from 2 up to 2.5 of Cu (%wt.), and based on Katgerman criterion, the normalized HCS value decreases from 1 up to 1,5 of Cu (%wt.), it increases from 1,5 up to 2 of Cu (%wt.), and it decreases from 2 up to 2.5 of Cu. In Fig. 7b, based on Feurer and SKK criteria, it shows that the normalized HCS value increases with Mg content (%wt.), based on Clyne &

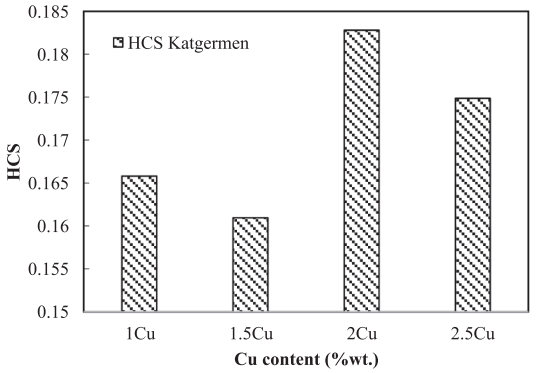

a)

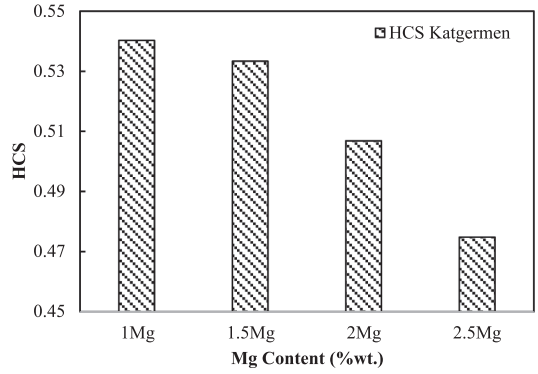

b)

Fig. 5. The HCS curve based on Katgerman criterion, (a) Al9Zn2Mg(1, 1.5, 2, 2.5 %wt.)Cu, and (b) Al9Zn(1, 1.5, 2, 2.5 %wt.)Mg2Cu.

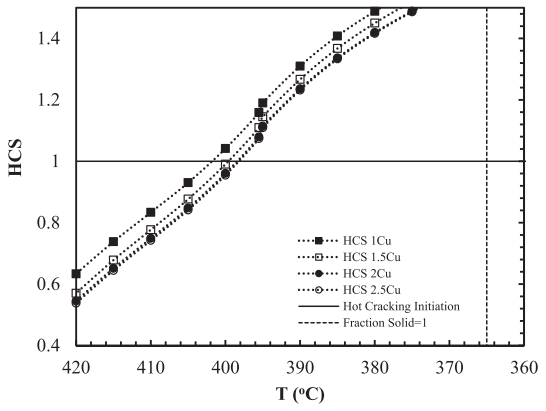

a)

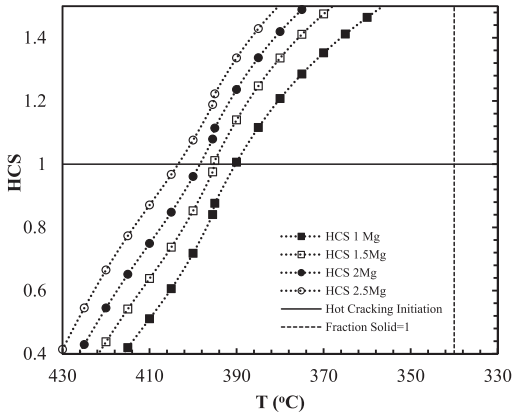

b)

Fig. 6. The HCS curve based on SKK criterion (a) Al9Zn2Mg(1, 1.5, 2, 2.5%wt.)Cu, and (b) Al9Zn(1, 1.5, 2, 2.5%wt.)Mg2Cu.

Davies criterion, the normalized HCS value decreases with Mg content from 1 up to 2 of Mg (%wt.), and it remains constant from 2 up to 2.5 of Mg (%wt.). Based on Katgerman criterion, the normalized HCS value decreases sequentially with Mg content.

Based on Fig. 7a-b, the HCS of some criteria are matched each other, and the HCS of some criteria are mismatched each other. Fig. 7a shows that the HCS of SKK is matched with the HCS of Feurer criterion for all varied Cu content, and the HCS of SKK and Feurer is matched with HCS of Clyne & Davies for some specific range of Cu content. HCS of Katgerman is mismatched with HCS of SKK, Katgerman, and Clyne & Davies for all varied of Cu content in Al9Zn2MgxCu alloys. Based on Fig. 7b, it shows that the HCS of SKK is matched with the HCS of Feurer criterion for all varied Mg content, and the HCS of Clyne & Davies is matched with the HCS of Katgerman for some specific range of Mg content in Al9ZnxMg2Cu alloys. It shows that the HCS of SKK and Feurer is mismatched with the HCS of Clyne & Davies and Katgerman. The reasons for matched and mismatched of the HCS of criteria are due to the considered parameters in the equation. SKK and Faurer have the same considered parameters for evaluating the HCS such as feeding, shrinkage, and deformation during solidification, thus SKK and Feurer is matched for all varied Mg and Cu content in in Al9Zn(x)Mg2Cu and Al9Zn2Mg(x)Cu alloys, respectively. Clyne & Davie considers the vulnerable time (t_v) and the time where the mass feeding and the liquid feeding occur (t_R). The t_v considers the time when the fraction of solid is 0.99 ($t_{0.99}$) and time when the fraction of solid is 0.9 ($t_{0.9}$), and the t_R considers the time when the fraction of solid is 0.9 ($t_{0.9}$) and when the fraction of solid is 0.4 ($t_{0.4}$). The Katgerman criterion considers the time when the feeding process is inadequate (t_{cr}) and the time when the coherency points during the solidification (t_{coh}). The t_{cr} is evaluated from the volumetric flow rate per unit volume *(SPV)* and shrinkage rate *(SRG)*.

Fig. 8a shows the crack length evaluated from the superheating effect and Cu content (%wt.) on the HCS of Al Alloys, and Fig. 8b shows the crack length evaluated from the superheating effect and Mg content (%wt.) on the HCS of Al alloys. The curves are generated from the experimental result. Generally, Fig. 8a shows that HCS increases with Cu content from 0 up to 0.5 of Cu (%wt.), it decreases from 0.5 up to 2 of Cu (%wt.), and it increases with Cu content from 2 up to 3 of Cu (%wt.) that is superheated at 100 °C (○), and it remains constant from 2 up to 3 of Cu (%wt.) that is superheated 20 °C (□). The results that are superheated at 100 °C (○) correlate to the Feurer and Clyne & Davies criteria, and the results that are superheated at 20 °C (□) correlate to SKK criterion. Fig. 8b shows that the HCS value increases from 0 up to 1 of Mg (%Mg.), and it decreases when the Mg content is more than 1 of Mg (%wt..). Generally,

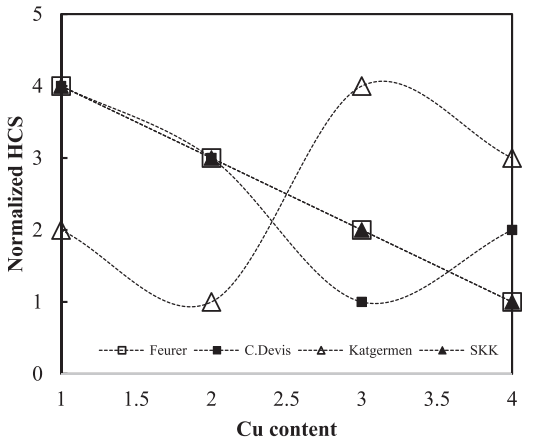

a)

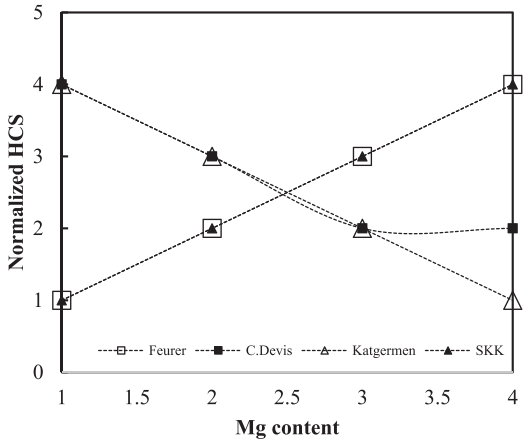

b)

Fig. 7. The normalized of HCS value based on Feurer, Clyne and Davies, Katgerman, and SKK criteria (a) Al9Zn2Mg(1, 1.5, 2, 2.5%wt.)Cu, and (b) Al9Zn(1, 1.5, 2, 2.5%wt.)Mg2Cu.

the results are in agreement with the Katgerman criterion, and it is in agreement with Clyne & Davies for 2 up to 2.5 of Mg (%wt.).

Figs. 9-10 show the other experimental result. Fig. 9 has a similar phenomenon to experimental data as in Fig. 8a where the HCS decreases with Cu content from 0 up to 2 of Cu (%wt.), and it increases from 2 up to 3 of Cu (%wt.). Fig. 9 uses the Cracking Susceptibility Coefficient* (CSC*) term to define the HCS value. Fig. 10 also has similar phenomenon to experimental data as in Fig. 8b where the HCS decreases from 1.5 up to 2.5 of Mg (%wt.). It can be stated that the Feurer, Clyne & Davies, and some specific range for SKK criteria are in agreement for the effect of Cu content (%wt.), and Katgerman and some specific range for Clyne&Davies criteria are in agreement for the effect of Mg content (%wt.).

Based on the results of the evaluation, it can be stated that more development of the model to predict the hot cracking as a function of chemical composition is still needed to be done as well as in the casting [44,45] and welding process [6,46,47].

4. Conclusions

Evaluation of the chemical composition on hot cracking susceptibility (HCS) using Feurer criterion, Clyne & Davies criterion, and Katgerman as non-mechanical criteria, and using SKK criterion as combined mechanical and non mechanical hot cracking criteria were studied. Based on Feurer criterion, The hot cracking initiates at lower temperature and at higher critical rate of feeding and shrinkage with Cu content, and the hot cracking initiates at higher temperature with Mg content, and it initiates at higher critical rate of feeding and shrinkage from 1 up to 1.5 of Mg, and the critical rate of feeding and shrinkage remains constant from 1.5 up to 2.5 of Mg. Based on Clyne & Davies, the HCS decreases with Cu content from 1 up to 2 of Cu, and it increases from 2 up to 2.5 of Cu. The HCS decreases with Mg content from 1 up to 2 of Mg, and it remains constant from 2 up to 2.5 of Mg. Based on Katgerman criterion, the HCS decreases with

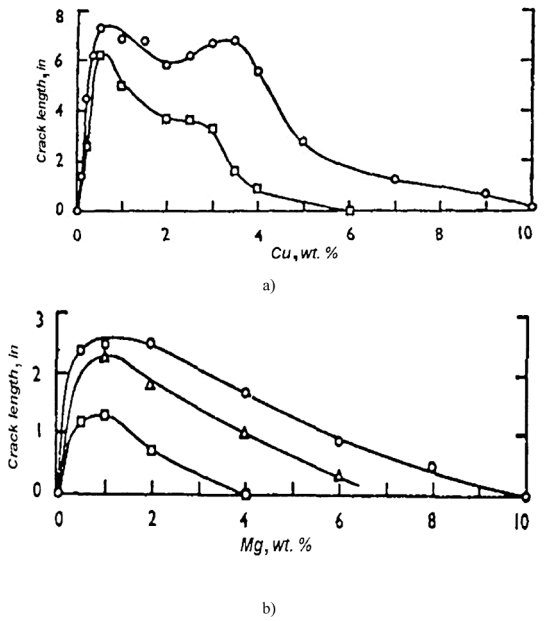

Fig. 8. The crack length evaluated from: a) the effect of superheating 100 °C (○) 20 °C (□) and Cu content (%wt.), and b) the effect of superheating 100 °C (○) 60 °C (Δ) 20 °C (□) and Mg content (%wt.) [19].

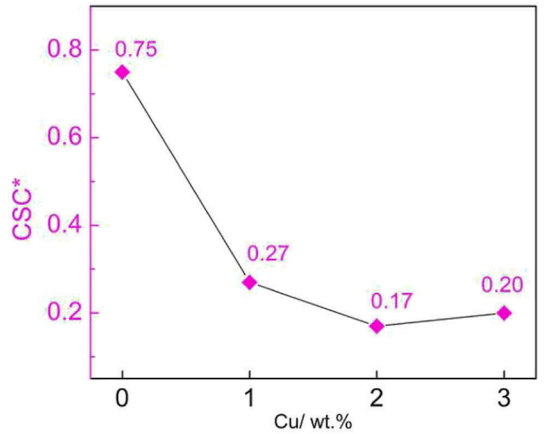

Fig. 9. The effect of Cu content on the HCS values on Al6Zn1.5 Mg(0, 1, 2, and 3 %wt.)Cu alloys [35].

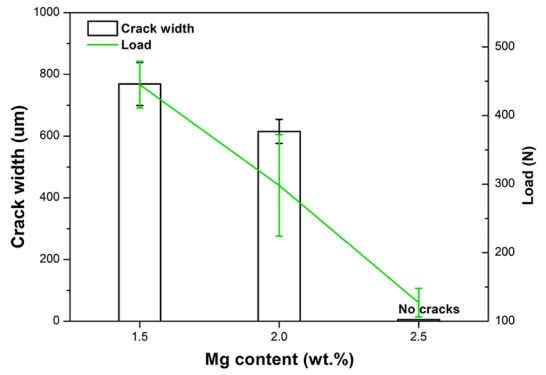

Fig. 10. The effect of Mg content on HCS value for Al9Zn(1.5, 2, 2.5 %wt.)Mg2Cu. [36].

Cu content from 1 up to 1.5 of Cu, it increases from 1.5 up to 2 of Cu, and it decreases from 2 up to 2.5 of Cu. The HCS decreases sequentially with Mg content. Based on SKK criterion, the HCS curves shift to the right with Cu content which means that the hot cracking initiates at lower temperature, and the HCS curves shift to the left with Mg content which means that the hot cracking initiates at higher temperature with Mg content. The Feurer, Clyne & Davies, and some specific range for SKK criteria are in agreement for the effect of Cu content on HCS of alloys, and Katgerman and some specific range for Clyne & Davies criteria are in agreement for the effect of Mg content on HCS of alloys. The intersection points between SPV and SRG curve indicate the critical temperature of each alloy during solidification. It occurs when the SPV is equal to SRG, and it implies the insufficient feeding process during solidification.

Declaration of Competing Interest

The authors declare that they have no known competing financial interests or personal relationships that could have appeared to influence the work reported in this paper.

Data availability

Data will be made available on request.

Acknowledgement

Authors would like to thank to Institut Teknologi Sumatera (ITERA) for providing the research grant (No. 631ah/IT9.2.1/PT.01.03/2023) through “Hibah Penelitian ITERA 2023”

References

[1] J. Campbell, Casting, Butterworth Heinemann, Oxford, 1991.
[2] S. Li, D. Apelian, Hot tearing of aluminum alloys: a critical literature review, International Journal of Metal Casting 5 (1) (2011) 23–40.
[3] H. Suyitno, tearing and deformation in direct-chill casting of aluminum alloys, Delft University of Technology, Netherland, 2005.
[4] J. Campbell, Complete Casting Handbook: Metal Casting Process, Metallurgy, Techniques and Design, in: Complete Casting Handbook, Elsevier, 2011, pp. 939–1011.
[5] C. Han, P. Jiang, S. Geng, S. Gao, G. Mi, C. Wang, Multiphase-field simulation of grain coalescence behavior and its effects on solidification cracking susceptibility during welding of Al-Cu alloys, Materials & Design 211 (2021), 110146.
[6] M.N. Jamesa, L. Matthews, D.g., Hattingh “Weld solidification cracking in a 304L stainless steel water tank”, Engineering Failure Analysis 115 (2020), 104614.
[7] Z. Gao, Y. Yang, L. Wang, B. Zhou, F. Yan, Formation mechanism and control of solidification cracking in laser-welded joints of steel/copper dissimilar metals, Metal, 12, 1147, 2022.
[8] C. Xia, S. Kou, Evaluating susceptibility of Ni-base alloys to solidification cracking by transverse-motion weldability test, Sci. Technol. Welding Join. 15(8) (2020) 1-8.
[9] C. Xia, S. Kou, Calculating the susceptibility of carbon steels to solidification cracking during welding, Metall. Mater. Trans. B 52 (1) (2021) 460–469.
[10] Y. Li, H. Li, L. Katgerman, Q. Du, J. Zhang, L. Zhuang, Recent advances in hot tearing during casting of aluminum alloys, Progr. Mater. Sci. 117 (2021).
[11] I.I. Novikov, Goryachelomkost tsvetnykh metallovi splavov (hot shortness of non-ferrous metals and alloys) 299, 1966.
[12] C.H. Dickhaus, L. Ohm, S. Engler, Mechanical properties of solidifying shell of aluminum alloys, AFS Transaction 101 (1994) 677.
[13] D.J. Lahaie, M. Bounchard, Physical modeling of the deformation mechanisms of semisolid bodies and a mechanical criterion for hot tearing, Metall. Mater. Trans. B 32 (2001) 697.
[14] J. Langlais, J.E. Gruzleski, A novel approach to assessing the hot tearing susceptibility of aluminum alloy, Mater. Sci. Forum 1 (2000) (2331-2337),167-172.
[15] J.A. Williams, A.R.E. Singer, Deformation, strength, and fracture above the solidus temperature, J. Inst. Met. 96 (1968) 5–12.
[16] Suyitno, W.H. Kool, L. Katgerman, Hot tearing criteria evaluation for direct-chill casting of an al-4.5 pct Cu alloy, Metall. Mater. Trans. A 36 (6) (2005) 1537–1546.
[17] W.H. Kool Suyitno, L. Katgerman, Evaluation of mechanical and non-mechanical hot tearing criteria for dc casting of an aluminum alloy, Light Metals, 753-758, 2003.
[18] L.Y. Zhao, Baoyin, N. Wang, V. Sahjwalla, R.D. Pehlke, The rheological properties and hot tearing behavior of an Al-Cu alloy, Int. J. Cast Met. Res. 13(3) (2000) 167-174.
[19] D.G. Eskin, Suyitno, L. Katgerman, Mechanical properties in the semi-solid sate and hot tearing of aluminum alloys, Progr. Mater. Sci. 49 (2004) 629–711.
[20] N.N. Prokhorov, resistance to hot tearing of cast metals during solidification, Russian Cast. Product. 2 (1962) 172–175.
[21] M. Rappaz, J.M. Drezet, M. Gremaud, A new hot tearing criterion, Metall. Mater. Trans. A 30 (2) (1999) 449–455.
[22] M. Braccini, C.L. Martin, M. Suéry, Y. Bréchet, modeling of casting Welding and Advanced Solidification Processes IX, 18-24, 2000.
[23] M. M’Hamdi, A. Mo, H.G. Fjær, TearSim, A two-phase model addressing hot tearing formation during aluminum direct chill casting, Metall. Mater. Trans. A, 37 (2006) 3069–3083.
[24] A. Stangeland, A. Mo, Ø. Dielsen, D. Eskin, M. Mhamdi, Development of thermal strain in the coherent mushy zone during solidification of aluminum alloys, Metall. Mater. Trans. A 35 (2004) 2903.
[25] T. W. Clyne, G.J. Davies, Solidification and casting of metals, The Metals Society (1979) 275-278.
[26] L. Katgerman, A mathematical model for hot cracking of aluminum alloys during dc casting, J. Met. 34 (2) (1982) 46–49.
[27] Suyitno, W.H. Kool, L. Katgerman, Integrated approach for prediction of hot tearing, Metall. Mater. Trans. A 40 (10) (2009) 2388–2400.
[28] Q.L. Bai, J.C. Liu, H.X. Li, Q. Du, L. Katgerman, J.S. Zhang, L.Z. Zhuang, A modified hot tearing criterion for direct chill casting of aluminum alloys, Mater. Sci. Technol. 32 (8) (2015) 1–9.
[29] M.A. Easton, H. Wang, J. Grandfield, C.J. Davidson, D.H. StJohn, L.D. Sweet, M.J. Couper, Observation and prediction of the hot tear susceptibility of ternary Al-Si-Mg alloys, Metall. Mater. Trans. A 43 (9) (2012) 3227–3238.
[30] L. Sweet, J. Taylor, M. Easton, M. Couper, N. Parson, Chemical additions to reduce hot tearing in the cast house. Light Metals: Springer International Publishing (2012) 1133–1138.
[31] A.A. Griffith, The theory of rupture, In: Proc., Ist., Int., Congr., Appl., Mech. Biereno, C.B. Burgers, J.M(eds). Delft: Tech. Boekhandel en Drukkerij. J. Waltman Jr, 54-63.
[32] A.A. Griffith, The phenomena of rupture and flow in solids, Philos. Trans. Roy. Soc. Lond. 221 (1921) 163–198.
[33] U. Feurer, Quality Control of Engineering Alloys and the Role of Metals Science, Delft University of Technology, Delft, 1997, 131.

[34] Y. Li, Z.R. Zhang, Z.Y. Zhao, H.X. Li, L. Katgerman, J.S. Zhang, L.Z. Zhuang, Effect of main elements (Zn, Mg, and Cu) on hot tearing susceptibility during direct-chill casting of 7xxx aluminum alloys, Metall. Mater. Trans. A 50 (8) (2019) 3603–3616.
[35] Y. Chen, Z. Liu, S. Liu, H. Guo, J. Liu, X. Sheng, Effect of Cu on the hot tearing susceptibility of Al–6Zn–2.5Mg–xCu alloy, Int. J. Metalcasting 15 (1) (2021) 130–140.
[36] W. Kurz, D.J. Fisher, Fundamentals of solidification, Trans Tech Publications, Switzerland, 1992.
[37] Y.S. Touloukian, E.H. Buyco (Eds.), Specific Heat, Springer US, Boston, MA, 1970.
[38] E. Suyitno, B. Pujiyulianto, M. Arifvianto, U.A. Mahardika, Salim,, Evaluation of quantitative hot cracking criteria, Mater. Sci. Technol. 38 (5) (2022) 269–280.
[39] D.G. Eskin, L. Katgerman, A quest for a new hot tearing criterion, Metall. Mater. Trans. A 38 (7) (2007) 1511–1519.
[40] M.H. Ghoncheh, S.G. Shabestari, A. Asgari, M. Karimzadeh, Nonmechanical criteria proposed for prediction of hot tearing sensitivity in 2024 aluminum alloy, Trans. Nonferrous Met. Soc. China 5 (28) (2018) 848–857.
[41] M.H. Ghoncheh, S.G. Shabestari, effect of cooling rate on the dendrite coherency point during solidification of Al2024 alloy, Metall. Mater. Trans. A 46 (3) (2015) 1287–1299.
[42] S.G. Shabestari, M.H. Ghoncheh, Investigation on the effect of cooling rate on hot tearing susceptibility of Al2024 alloy using thermal analysis, Metall. Mater. Trans. B 46 (6) (2015) 2438–2448.
[43] L. Fa-Guo, D. Qing, Z. Jiao, D. Yong-Bing, F. Ya-Nan, X. Hong-Lan, Y. Fu-Cheng, S. Bao-De, in situ on columnar-equiaxed transition and an axial columnar dendrite growth of Al−15%Cu alloy by synchrotron radiography, Trans. Nonferrous Met. Soc. China, 24 (2014) 2112−2116.
[44] D. Warrington, D.G. Mccartney, Development of a new hot-cracking test for aluminium alloys, Cast Met. 2 (3) (1989) 134–143.
[45] Y. Zhu, K. Zhou, G. Xu, C. Xu, X. Li, Y. Li, B. Wang, F., Oppong "Crack formation of camshaft castings: hot tearing susceptibility and root causes", Eng. Failure Anal. 147 (2023), 107143.
[46] A. Almomani, A. Hamid I. Mourad, I. Barsoum, Effect of sulfur, phosphorus, silicon, and delta ferrite on weld solidification cracking of AISI 310S austenitic stainless steel, Eng. Fail. Anal. 139 (2022) 106488.
[47] M.N. James, L. Matthews, D.G. Hattingh, Weld solidification cracking in a 304L stainless steel water tank, Eng. Fail. Anal. 115 (2020) 104614.